ADVANCED FUNCTIONAL MATERIALS
www.afm-journal.de

www.MaterialsViews.com

Bright White Scattering from Protein Spheres in Color Changing, Flexible Cuttlefish Skin

Lydia M. Mäthger, Stephen L. Senft, Meng Gao, Sinan Karaveli, George R. R. Bell, Rashid Zia, Alan M. Kuzirian, Patrick B. Dennis, Wendy J. Crookes-Goodson, Rajesh R. Naik, George W. Kattawar, and Roger T. Hanlon*

Throughout nature, elegant biophotonic structures have evolved into sophisticated arrangements of pigments and structural reflectors that manipulate light in the skin, cuticles, feathers and fur of animals. Not many spherical biophotonic structures are known and those described are often angle dependent or spectrally tuned. White light scattering by the flexible skin of cuttlefish (*Sepia officinalis*) is examined and how the unique structure and composition of leucophore cells serve as physiologically passive reflectors approximating the optical properties of a broadband Lambertian surface is investigated. Leucophores are cells that contain thousands of spherical microparticles called leucosomes that consist of sulfated glycoproteins or proteoglycans and reflectin. A leucophore containing ≈12 000 leucosome microspheres is characterized three-dimensionally by electron microscopy and the average refractive index of individual leucosomes is measured by holographic microscopy to be 1.51 ± 0.02. Modeling of the ultrastructural data and spectral measurements with Lorenz-Mie theory and Monte Carlo simulations suggest that leucophore whiteness is produced by incoherent scattering based upon a randomly ordered system. These soft, compliant, glycosylated proteinacious spheres may provide a template for bio-inspired approaches to efficient light scattering in materials science and optical engineering.

1. Introduction

An object's hue results from structural or pigmentary coloration, and whiteness is created by equal scattering of all visible wavelengths.[1] Structural coloration involves colorless materials that create colors by scattering, whereas pigmented materials have selective absorbance that limits the spectral redistribution of light incident on an object. Patterns with white are common in vertebrates and invertebrates, and play key roles in camouflage and signaling by increasing the achievable degree of contrast.[2–4] There has been widespread interest in biophotonic structures that create white coloration. The white structures that have been described in detail are mainly from insects,[4–7] and in particular, the scales of the beetles *Cyphochilus, Lepidiota stigma* and *Calothyrza margaritifera*.[4,7] While there are some examples of very high reflectance,[7] these structures often reflect less strongly at oblique angles.[5,6] Recently, Luke et al.[7] used microscopy, spectrophotometric and theoretical modeling techniques to show that the rigid microstructures in beetle scales are optimized to scatter light, resulting in brilliant whiteness.

We focused on the flexible skin of a marine mollusc, the European cuttlefish, *Sepia officinalis,* that uses organic spheres inside cells known as "leucophores" to produce diffuse bright white scattering (**Figure 1**). Cuttlefish are capable of rapid adaptive coloration that produces effective camouflage against predation as well as high-contrast signaling displays for conspecifics.[8] For example, the zebra stripe display of male cuttlefish (Figure 1B) is especially prominent during male aggression. This high-contrast light and dark pattern depends upon the expression of dark brown stripes created by fully expanded dark chromatophores, interleaved with bright white zebra stripes containing leucophores (with overlying chromatophores retracted). To modify the contrast of the stripes (or to eliminate them) the cuttlefish expands chromatophores over the white stripes of leucophores while simultaneously retracting (to variable and controllable levels) the chromatophores in the adjacent stripes. The same pattern can then become a low-contrast "weak Zebra pattern" that is effective in camouflage on appropriate backgrounds.[8] The switch from highly conspicuous

L. M. Mäthger, S. L. Senft, G. R. R. Bell, A. M. Kuzirian, R. T. Hanlon
Marine Biological Laboratory
Program in Sensory Physiology and Behavior
Woods Hole, MA 02543, USA
E-mail: lmathger@mbl.edu

M. Gao, G. W. Kattawar
Institute for Quantum Science and Engineering
Department of Physics and Astronomy
Texas A&M University
College Station, TX 77843, USA

S. Karaveli, R. Zia
School of Engineering
Brown University
Providence, RI 02912, USA

P. B. Dennis, W. J. Crookes-Goodson, R. R. Naik
Soft Matter Materials Branch
Materials and Manufacturing Directorate
Air Force Research Laboratory
Wright-Patterson Air Force Base, OH, 45433, USA

R. T. Hanlon
Ecology and Evolutionary Biology
Brown University,
Providence, RI 02912, USA

DOI: 10.1002/adfm.201203705

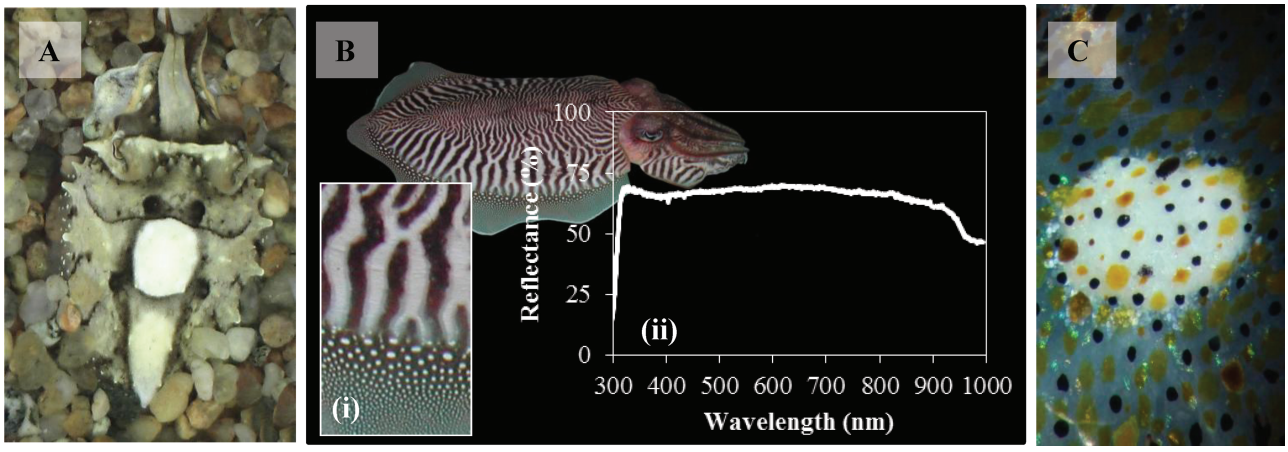

Figure 1. Cuttlefish, *Sepia officinalis*, are known for their fast color and pattern changes, in which pigmented chromatophores, innervated directly by the brain, work in concert with subjacent structural light reflectors (iridophores and leucophores).[48–50] When cuttlefish retract their pigmented chromatophores, white-scattering leucophores are exposed, creating white skin areas for camouflage and signaling. A) Cuttlefish (approximate length: 15 cm) in disruptive camouflage and B) showing signaling ("zebra") display. i) Enlarged fin with zebra stripes and fin spots; diameter of spots 2–5 mm. ii) Spectral reflectance of one highly reflective fin spot, showing broadband reflectance in the ultraviolet, visible and near infrared (approximately 70% from 300–1000 nm). C) Enlarged fin spot; ca. 3 mm diameter.

to well-camouflaged is accomplished in milliseconds by enhancing or masking the fixed stripes of leucophores in the skin via selective, fine-tuned neural control of the overlying pigmented chromatophores that are evenly distributed in the skin. In addition to dynamic pigmentary patterning, cuttlefish can rapidly morph their highly compliant skin into various shapes and protrusions.[9] Leucophores are flexible too, a feature that allows cuttlefish to show uniformly diffused white of varying contrasts for camouflage and signaling, even while changing their 3D shape.

Leucophores are located on the fin (see the bright white spots and lines in Figure 1B,C) as well as in other areas across the dorsal side of the body of cuttlefish and octopus.[8,10] Leucophores contain a large number of minute, reflective, irregularly packed spheres called leucosomes. Few such broadband spherical biological reflectors are described in the literature. The beetle *Pachyrhynchus* has chitinous, periodically arranged sphere-like units that produce angle-dependent green iridescence.[11] Randomly packed spheres are shown to produce a range of colors in the beetle *Anoplophora graafi*.[12] The system most analogous to cuttlefish is the white beetle *Calothyrza margaritifera,* which produces broadband white scattering by a tight packing of chitin spheres.[7] Although capable of producing structural coloration, chitin is stiff and inflexible, as it adds structural support to the insect's exoskeleton.

Industrial desire for soft, flexible, adaptive displays is promoting considerable interest in emulating natural systems,[13–15] particularly if better use can be made of ambient light[16,17] to decrease the need for electrical power. The biological photonic system of cuttlefish may find useful applications in optical technology and engineering, as it is flexible and requires no energy input once formed.

In the following, we present a detailed investigation of the optical properties, structure, and composition of *Sepia officinalis* fin spots, which have the brightest reflectance compared to other white areas on the animal's body. From whole skin samples, we measured reflectance and observed angle- and polarization-independent broadband (white) light scattering. To understand the biological origin of this effect, we used a variety of methods to investigate the structure and composition at decreasing length scales. We employed 3D, serial block-face scanning electron microscopy to characterize the microstructure of a complete leucophore. This technique involved serially sectioning (50 nm) an epoxy embedded fin spot and, using high resolution scanning electron microscopy (SEM), collecting images of the block face after each section was removed. We then used holographic analysis to determine the effective refractive index of individual leucosomes. Using this information, we numerically simulated the scattering response of cuttlefish skin and compared theoretical results to experimental measurements. We also performed proteomic analysis of dissected fin spots and isolated leucophores to identify the constituent materials that enable this unique broadband biological reflector.

2. Results

2.1. Spectral Reflectance Measurements and Physiological Studies

The fin spots of *Sepia officinalis* reflect light across the ultraviolet, visible and near infrared (300–1000 nm; Figure 1B,ii). Spectral reflectance, measured with Ocean Optics spectrometers, ranged from ca. 30% to ca. 75% (average of ca. 45%; **Figure 2**A; see Experimental Section for details on methodology). This reflectance range is most likely due to thickness variations of fin spots. Thicker fin spots of larger animals, or fin spots located closer to the animal's body, reflected more strongly, while the opposite was true for fin spots on the periphery of the fin or in

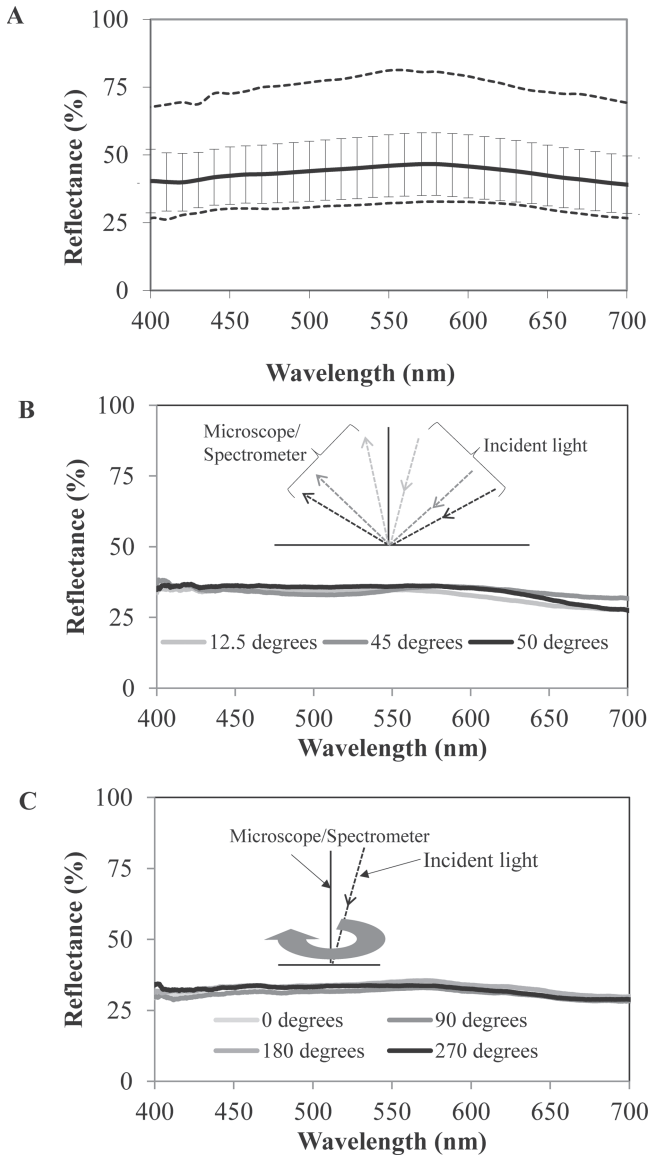

Figure 2. A) Reflectance (from 400–700 nm) of fin spots relative to a white standard ranged from approximately 30% to 70%. Larger animals have larger and thicker fin spots and higher reflectance. Plot shows average fin spot reflectance and standard deviations (measured from 50 fin spots, total of seven animals). Dashed lines are maximum and minimum measured reflectance values ($n = 50$). Fin spots containing leucophores approximate a Lambertian surface, reflecting the same amount of light in all measured directions. B) Spectral reflectance measurements (from 400–700 nm) of leucophores in intact cuttlefish skin in vertical plane. Angles of illumination and viewing (in water at the skin surface) were 12.5°, 45° and 50°. C) Spectral reflectance measurements (from 400–700 nm) in horizontal plane; preparation rotated from 0° to 90°, 180° and 270°. Incident angle in water at skin surface: ca. 8°. Slight variations are due to movement of the live skin.

smaller animals. We observed thicknesses for fin spots at the fin's periphery ranging from ca. 100 μm to ca. 300 μm. The highest reflectance values were from large animals for which we have no thickness measurements, so the upper range of fin spot thickness likely exceeds 300 μm. The intensity of reflected white light was equal when viewed from multiple angles and when illuminated from multiple incident angles (Figure 2B,C). This approximates the definition of a Lambertian surface,[1] at least up to angles of approximately 50° incidence.

Cuttlefish leucophores are flexible and, although not quantified, do not appear to lose their diffuse optical properties when physically deformed and manually manipulated (e.g., cut, stretched or dried). Leucophores are not associated with nerves or muscle fibers and are physiologically inactive. To verify this, bioactive compounds known to elicit cellular changes in the structures involved in color change in cephalopods and fish were tested. These included: KCl and noradrenaline, both known to change reflectance in some fish iridophores;[18] acetylcholine, known to change reflectance in squid iridophores;[19] and L-glutamate and 5-HT, both involved in chromatophore muscle physiology.[20] Reflectance remained the same throughout the incubation time for all compounds tested (Figure S1, Supporting Information).

2.2. Morphology Studies

Details were derived from a 3D data set consisting of 1500 serial electron microscopy images of fin spot tissue sections cut at a thickness of 50 nm (see Experimental Section for methodology). This volumetric image data set contained leucophores and iridophores (**Figure 3**A,B). A complete, single leucophore, measuring approximately 55 μm × 20 μm × 15 μm, was identified within a subset of these 3D serial images (Figure 3C). This cell was completely filled with spherical leucosomes except for a few cup-shaped inclusions, a centrally located, irregularly shaped nucleus, and a number of electron-lucent, membrane-bound inclusion bodies. A computer algorithm identified 11993 leucosomes with a diameter distribution ranging from 233 nm to 1967 nm (average: 759 nm ± 203 nm; Figure 3D). Spheres below a diameter of ca. 300 nm were difficult to measure, and may not be represented fully in our data set. However, their exclusion is not expected to significantly impact the simulation results presented here.

From our morphology studies, we were able to obtain a leucosome number density (n_d, defined as the number of leucosomes in a unit volume inside of a leucophore), estimated to be approximately 1 μm^{-3}. Leucosomes are distributed uniformly along all three cardinal axes (Figure S2, Supporting Information). By volume, leucosomes comprised at least 35% of this leucophore. Note that the theoretical maximum packing of an irregular collection of spheres is 63%.[21] The remaining cell volume consisted of the nucleus (approximately 4%) and cytoplasm. From these data, we found that the volume fraction for platelets in iridophores was also approximately 35%. Looking at the entire fin spot, the packing of leucophores plus iridophores was approximately 80% by volume. Consequently, the fin spot as an optical system consisted of at least 28% (35% × 80%) reflecting material (platelets plus spheres).

2.3. Holographic Characterization of Individual Leucosome Size and Refractive Index

Having characterized the structure of a single leucophore, we investigated the optical properties of individual leucosomes. To

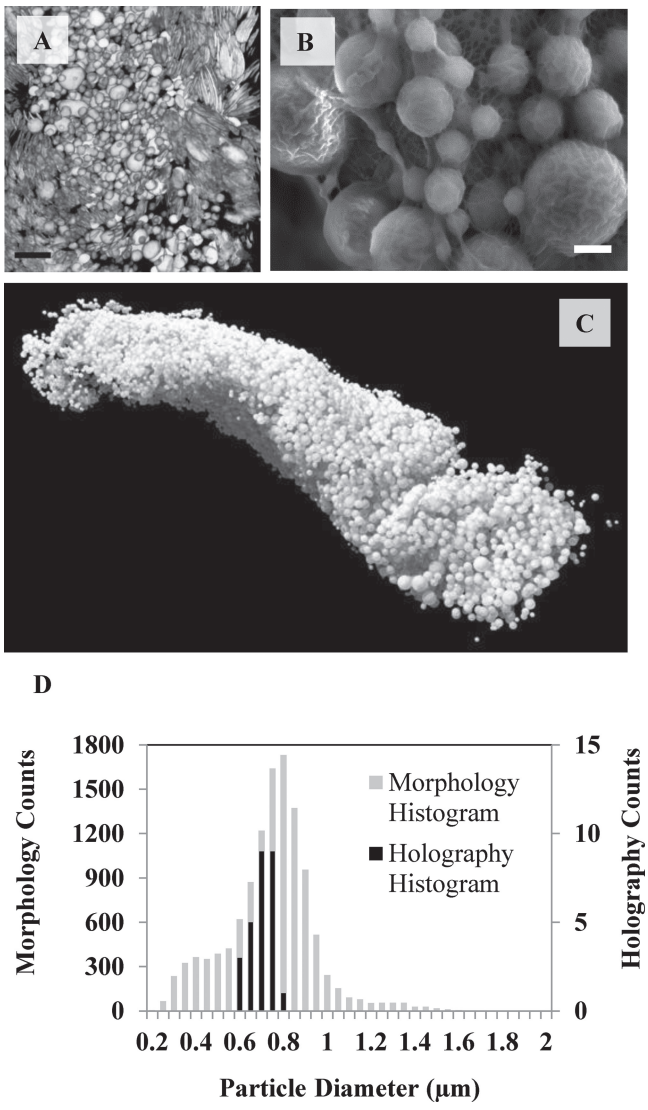

Figure 3. A) Volume rendering of a subset of the 3D electron microscopy data (see Experimental Section for details), showing packing of leucosomes within a single leucophore. Surrounding platelets are from adjacent iridophores. Scale: 2 μm. B) SEM image of spherical leucosomes. Scale: 500 nm. C) 3D rendering of approximately 750 serial (50 nm thickness) SEM images acquired using the Gatan, 3View System. Centrally located leucophore (dimensions: 55 μm × 20 μm × 15 μm) contains spherical leucosomes. D) Histogram of leucosome size distribution (diameter) of the approximately 12 000 spheres shown in (Figure 3C). Also shown are the size distributions of 27 leucosomes used to determine refractive index by the holographic method (see Figure 4).

this end, leucophores were harvested from fin spot samples and placed in deionized water between a microscope slide and coverslip with a thin spacer (≈150 μm). This allowed the free movement of individual leucosomes by Brownian motion when the leucophores burst (either under osmotic pressure or with the assistance of optical tweezers). The effective refractive index and size of individual leucosomes was then determined by in-line digital holographic microscopy, which has been previously used to track and characterize single spherical dielectric particles[22] and infer their porosities.[23] Such holographic techniques have also been used to determine the refractive index of biological samples, including milk fat globules[24] and fish reflectors.[25]

Multiple holographic images were recorded for each freely diffusing leucosome and fit to Lorenz-Mie theory using software developed by the Grier lab.[22–24,26] Digital holograms were acquired for 27 distinct spherical particles from the leucophore sample preparation (see Experimental Section for methodology). Particles that were plate-like (i.e., indicative of iridophore material) were excluded from the analysis. In total, 7026 holograms were analyzed, yielding an average diameter of 704 nm ± 54 nm and effective refractive index of 1.51 ± 0.02. **Figure 4** shows the refractive index and size distribution characterized for each leucosome with associated standard deviation. As shown in Figure 3D, the particle size distribution measured from aqueous leucosomes by in-line holography is consistent with the size distribution obtained by the 3D electron microscopy method, and thus helps to validate the ultrastructure data on fixed samples as accurate representatives of the aqueous tissue.

2.4. Simulation

Leucophores consist of a large collection of leucosomes (Figure 3C). When light enters a leucophore, the leucosomes scatter the light multiple times before it is finally reflected back.

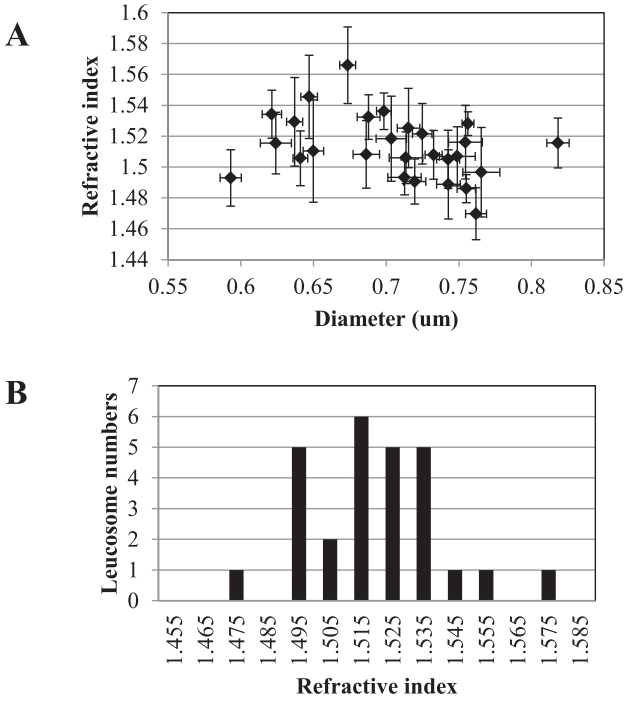

Figure 4. A) Measured refractive index and radius for 27 individual leucosomes. Average refractive index: 1.51 ± 0.02. Each spot corresponds to the mean refractive index and radius of an individual leucosome, averaged over all the measured holograms belonging to that particle. The error bars show the standard deviation for measured values from each leucosome. B) Histogram showing distribution of measured refractive indices shown in (A).

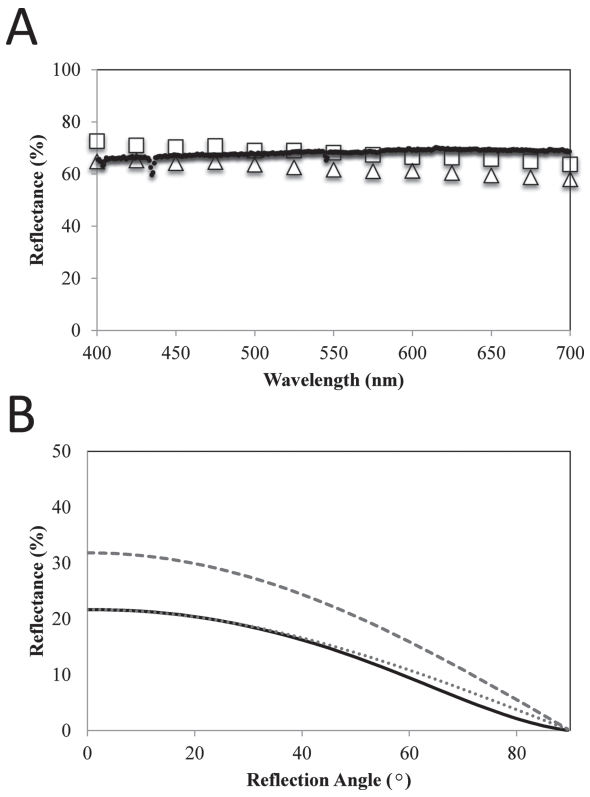

Figure 5. Simulations show that fin spot system approximates a Lambertian surface. A) Dots: Measured reflectance (from 400–700 nm) from cuttlefish fin spot can be as high as ca. 70%, reflecting equally well across the visible spectrum. Triangles: modeled flux reflectance spectrum averaged over all reflection angles and for 0° incidence. Squares: the normalized reflectance spectrum obtained by normalizing the modeled reflectance to a perfect Lambertian reflector (shown in (B)) at the same 0° incident and reflection angle, which is commensurate with the measurement. The normalized reflectance averaged over the visible spectrum is chosen to be the same as the measurement (both are 68%). B) Modeled angular reflectance averaged over the visible spectrum. The modeled angular distribution (solid line) is close to a cosine function (represented by the dotted line) typical of a Lambertian surface. The dashed line is the angular distribution ($\cos\theta/\pi$) of a perfect Lambertian surface, which has a 100% total reflectance integrated over 2π solid angle.

Fundamentally, the optical paths taken by the photons depend predominantly on how an individual leucosome scatters light.

Using the Monte Carlo method (see Experimental Section), the reflectance at a given incident and reflection angle was calculated and normalized to the reflectance (at the same angle) of a Lambertian reflector that reflects 100% of the incident light. The resulting normalized reflectance was compared to the measured reflectance in **Figure 5**A. Since the corresponding thickness and number density were not available, to compare the shapes of these two spectra, the normalized reflectance averaged over the visible spectrum was chosen to be the same as the measured results of 68%. To produce this reflectance, the product of number density and system thickness in the simulation n_dL is 64 μm^{-2}. Both the experimental and simulated reflectance spectra shown in Figure 5A exhibit a similar flat spectral response. The flux reflectance averaged over all reflection angles (with no normalization) was also calculated and compared with the normalized reflectance spectra. Both spectra are similarly flat but there is a 10% magnitude difference due to the slight angular difference between the simulated and Lambertian reflectance (Figure 5B). The normalized reflectance is a little higher than the measurement at shorter wavelengths, but is lower at longer wavelengths; this difference may come from the contribution of iridophore plates, which were not considered in our modeling.

The simulated angular distribution of the reflectance at 0° incidence is shown in Figure 5B. The reflectance has been averaged over the entire visual spectrum and is found to be independent of the azimuthal angle. The angular reflectance distribution is close to a cosine function, and it implies that the simulated fin spot system acts as a good Lambertian reflector according to Lambert's cosine law. Additionally, our simulation shows that polarization is negligible (less than 10%) over the whole visual spectrum, which agrees with spectral reflectance data of intact tissue (Figure S3, Supporting Information). These results confirm the bright white diffuse reflectance of the fin spot system and suggest that incoherent multiple scattering is sufficient to produce it.

2.5. Protein Analysis

Basic histochemical staining helped determine the compositional components of leucosomes (**Figure 6**). When combined in sequence, Halmi's paraldehyde (basic) fuchsin and alcian blue (pH 2.5) (Figure 6A)[27] stained leucophores strongly purple indicating the presence of strongly acidic, sulfated mucoproteins (see Experimental Section for methodology). Positive leucophore staining with Müller's colloidal iron confirmed the presence of an associated sugar moiety (i.e., leucosomes contain glycoprotein or proteoglycan) (Figure 6B). Reflectin immunohistochemistry using antibodies directed against reflectins from the light organ reflector of the Hawaiian bobtail squid[34] showed preferential affinity of the antibody for iridophores, and weaker binding to leucophores (Figure 6C,D). Quantitative gray-scale measurements demonstrated stronger labeling on platelets (67.1 ± 2.2 s.e.) and less labeling on spheres (54.5 ± 1.6 s.e.).

Since the initial analysis of leucophores indicated a proteinaceous component, proteomic analysis was performed on material extracted from dissected, homogenized fin spots (see Experimental Section for methodology). After homogenization, the extracts appeared as a milky-white suspension that cleared during centrifugation, leaving a white pellet. Resolution of the fin spot-derived pellet by SDS-PAGE followed by staining with Coomassie blue indicated the presence of a number of protein species with a broad molecular weight distribution (Figure 6E). Each band of protein species was excised, digested with trypsin from the gel slice and analyzed using matrix-assisted laser desorption/ionization time-of-flight (MALDI-TOF) mass spectrometry and tandem mass spectrometry for sequence determination of select peptides. Analysis of each protein species indicated homology to a number of squid reflectin isoforms (Figure S4, Supporting Information). No non-reflectin-like proteins appeared to be present in the extracted fin spot pellets,

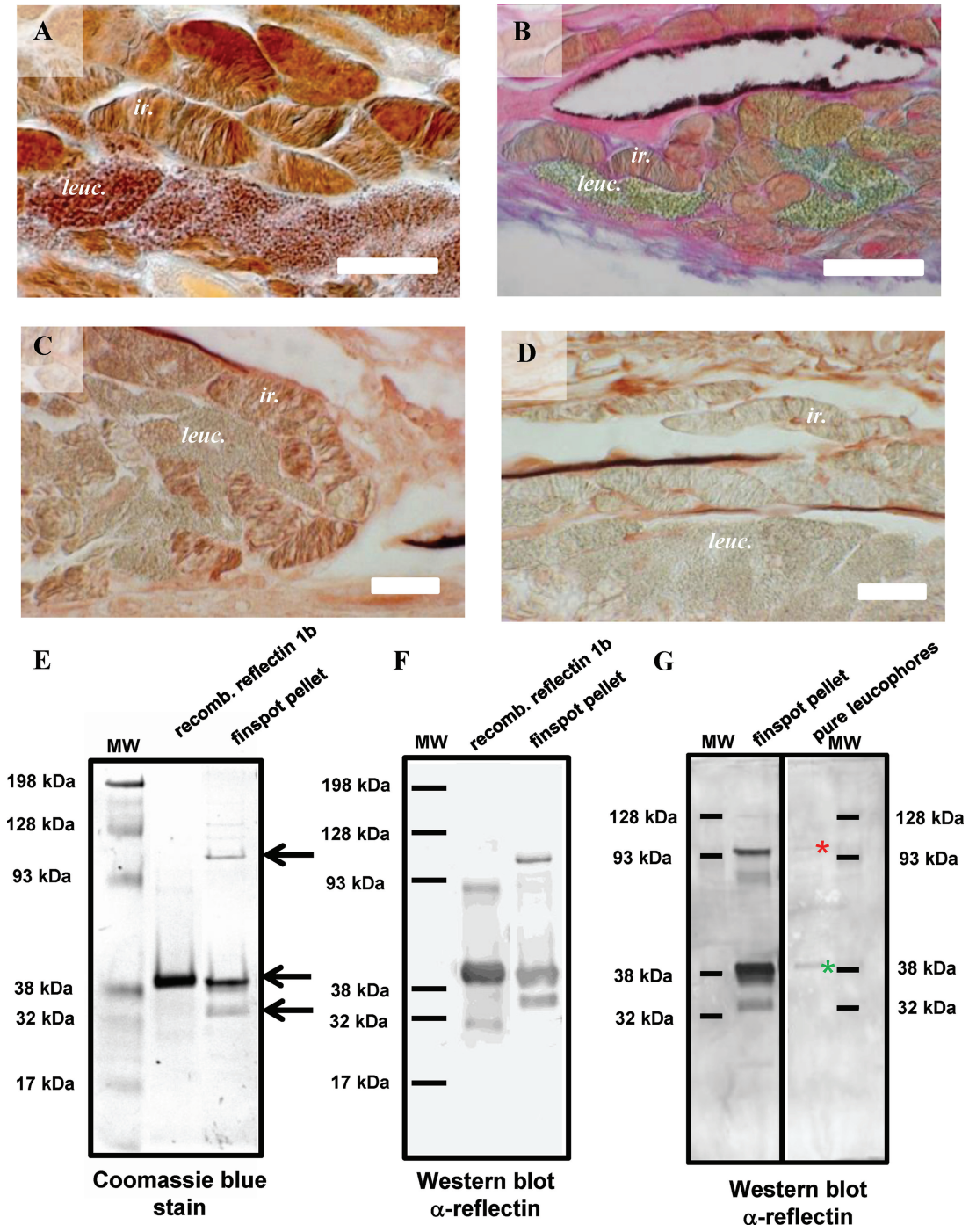

Figure 6. Leucophores (*leuc*) show preferential labeling over iridophores (*ir*) when stained with A) Aldehyde Fuchsin/Alcian blue (pH 2.5; purple/red spheres) and B) colloidal Iron (scale for (A,B): 10 µm; blue-green color). C) Sections labeled with anti-reflectin antibody and D) negative control (scale for (C,D): 20 µm). Degree of immunolabeling was quantified using grey-scale intensity measurements (Image-J). Anti- *E. scolopes* reflectin antibody labeling on positive (C) and negative control (D) slides was measured for iridophores, and leucophores (20 µm diameter circular regions; $n = 12$ each). Results indicated highest antibody affinity for iridophores (67.1 ± 2.2 s.e.) with less staining demonstrated by leucophores (54.5 ± 1.6 s.e.). Negative control intensities for the two cell types were 23.9 ± 1.2, and 30.5 ± 1.4, respectively. E) Coomassie blue stain of bacterially expressed, squid reflectin 1b and the insoluble fraction of extracted fin spot tissue after resolution by SDS-PAGE. The sizes of molecular weight (MW) markers are indicated on the left and arrows on the right indicate specific protein species in the fin spot sample analyzed by mass spectrometry. F) Recombinant reflectin 1b and the insoluble fin spot fraction were resolved with SDS-PAGE followed by Western blotting and probing with an anti-reflectin antibody (α-reflectin) from *E. scolopes*. Positions of molecular weight markers are indicated on the left. G) Purified leucophores were resolved in toto with SDS-PAGE followed by Western blotting and probing with the reflectin antibody (right panel). Green asterisk shows a 38 kDa reflectin-positive band, red asterisk indicates the location of an additional, 93 kDa, reflectin-positive band (weaker in comparison with others). A lane containing the insoluble fin spot fraction was added for direct comparison (left panel).

indicating that the cuttlefish reflectins identified were the dominant protein species in the insoluble fraction. Analysis of the clarified, soluble, fin spot material did not yield a dominant protein species (Figure S5, Supporting Information), and only comprised 13% of the total protein. Western blot analysis of the fin spot pellet proteins using a polyclonal antibody raised against *Euprymna scolopes* light organ reflectins (Figure 6F) confirmed the mass spectrometry results, indicating cross-reaction with all of the protein species observed with Coomassie Blue staining. The dominant cross-reacting protein migrated with an apparent molecular weight of ≈40 kDa; the molecular weight of squid reflectin. Interestingly, the anti-reflectin antibody also cross-reacted with a high molecular weight series of protein bands (at ≈110 kDa and higher) that mass spectrometry indicated were reflectin-like. Similarly sized reflectins were also observed in reflector tissue of the Hawaiian bobtail squid.[34] These results may indicate yet unidentified isoforms of reflectin may exist with higher molecular weights.

It is certain that the above-mentioned material, extracted from whole fin spots, also contained iridophores that associate closely with leucophores. To address this, collagenase treated and dispersed fin spots were sorted using microscopy at a magnification sufficient to distinguish cells containing spheres (leucophores) from those containing platelets (iridophores). Manual selection, using a laser-capture technique, yielded a small, highly enriched sample of leucophores. These cells were solubilized in SDS-PAGE sample buffer and directly analyzed by Western blotting using the anti-reflectin antibody (Figure 6G). A cross-reactive band was observed at the predicted molecular weight of squid reflectin (40 kDa), as well as at the higher 110 kDa band (red asterisk, Figure 6G). This indicates that cuttlefish proteins related to the squid reflectins are present in leucophores and may play a role in the formation and function of light scattering leucosomes. The biochemical finding of reflectins within the isolated leucophores is in good agreement with the results from histochemical staining of the tissue, which indicated the presence of a sulfur-containing glycoprotein or proteoglycan in leucophores. Methionine is the second most abundant amino acid in reflectins, representing ≈14% of the total amino acids.

3. Discussion

The biophotonic system of the cuttlefish leucophore fin spot has distinctive properties and microstructural mechanisms to produce whiteness ranging from the ultraviolet to the infrared. We were able to directly measure the effective refractive index of individual spherical leucosomes and found the average value to be 1.51 ± 0.02. Reflectance measurements and numerical simulations showed that leucophores act as a good Lambertian surface. The spatial correlation and the local coherency in some biophotonic systems can be important in producing color.[11,12,28–30] However, since leucosomes appear to be randomly positioned scatterers, the observed reflectance spectrum is uniformly white and diffuse. In nature, cuttlefish experience light fields that can be directional (e.g., on sunny days at shallow depth) or diffuse (e.g., at greater depth or on cloudy days).[31] Leucophores are structured effectively to suit a wide range of natural light fields by uniformly scattering incident light that is directional, diffuse or even polarized.

An interesting feature of the leucophore is its compliant nature, but work is needed to quantify how compliant it is. Materials researchers may use the cephalopod template when looking to design flexible (e.g., rollable or stretchable) displays. While other biophotonic structures have similar optical properties, such as the whiteness in beetles of the genera *Cyphochilus*, *Lepidiota* and *Calothyrza*,[4,7] their structures are brittle and delicate. Cuttlefish skin is renowned for being flexible, and the random scattering mechanism that underlies its broadband reflectance is insensitive to shape change. Certainly, a potential weakness in the cuttlefish system is that fin spots are comparatively thick (>100 μm), whereas the scales of the above-mentioned beetles can achieve comparable brightness levels while using much thinner structures (5–10 μm thick).[7] However, the beetle scales sacrifice flexibility and robustness.

Serial images of the fin spot ultrastructure yielded high-resolution 3D information concerning the spatial arrangement of both its leucophores and iridophores. The carefully segmented electron-microscopy data set provided an unprecedented view into a single cuttlefish leucophore. Analysis of the particle locations inside the leucophore suggested that the spatial arrangement of leucosomes is unordered and, thus, the entire cell may be modeled as a random system. We were then able to perform extensive optical modeling, which implied that incoherent scattering through multiple size leucosomes was sufficient to produce diffuse, bright white reflectance. We have not fully characterized the geometry of platelet iridophores in this fin spot system. However, despite the complex structures of iridophores, the fin spot, as an optical system, exhibits a similar spectrum to a uniform spherical leucosome system. This similarity suggests that the fin spot is a strongly multiple scattering system. Stacks of parallel iridophore plates are likely also randomly positioned and oriented, and as stacks behave optically in a similar manner to spherical leucosomes. When oriented accordingly, platelet-containing iridophores have been shown to reflect broadband, reasonably diffuse light.[32,33] Therefore, due to the strong multiple scattering, fin spots, as an optical system, can produce an angular reflectance distribution similar to a Lambertian surface.

Results of histochemical staining (particularly colloidal iron) suggest that the leucophores contain sulfated proteoglycans or glycoproteins. The fact that leucophores also contain reflectin proteins, which previously have only been characterized in iridophore cells,[33–35] suggests that this protein family may assist in manipulating light in multiple ways. How light is manipulated may depend on a number of factors such as the morphology of the organelle into which it is packaged (iridophore platelets or leucophore spheres) and organelle-specific post-translational modifications of the protein. Thus, it is possible that reflectins may be modified by post-translational glycosylation and sulfation. Holographic characterization also showed that the effective refractive index of aqueous leucosomes (n_r = 1.51) is lower than the index measured from recombinant squid reflectin (n_r = 1.59)[35]; this may be due to direct chemical differences in the biochemical composition or distinctions in how water infiltrates these materials.[23] The fact that leucosomes contain both protein and non-proteinaceous components (glycosylated

carbohydrates), suggests the possibility of extensive tunability, as proteins can be both genetically programmed, as well as post-translationally functionalized to generate novel properties. Such advantages are currently being exploited with silk proteins isolated from spiders and the silkworm, *Bombyx mori*.[36]

Cuttlefish leucophores may provide novel bio-inspiration in the fields of optical engineering and materials science. Light diffusers have important applications in a variety of optical devices, including color mixing for white-light LEDs and uniform back illumination for compact, high-quality displays (e.g.,[17]). The optical principles of light diffusion by leucophores may provide a non-synthetic proteinaceous alternative to commercially available titanium dioxides nanoparticles or polymer microspheres. The passive nature (no energy requirement), high reflectance, physical flexibility and efficient light diffusion of leucophores may have applications in reflective electronic displays that leverage ambient light.[16]

Nature presents many elegant biophotonic structures, and we are only beginning to appreciate the potential device applications that some of these structures can offer. The work of Kramer et al.[35] effectively highlights how bio-derived materials, particularly recombinant reflectin proteins from squid iridophores, may be used for photonic applications. In our study, we aimed to understand how similar materials are shaped and assembled to achieve a specific optical function in a biological system. Unlike the assembly of squid reflectin into ordered iridophore platelets for specular reflection, our detailed analysis has shown how random assemblies of spherical leucosomes containing sulfated glycoproteins or proteoglycans and reflectin produce broadband diffuse reflectance. We hope that further analysis of this and similar biological systems, by combining the advanced methods presented here, such as 3D electron-microscopy, holographic characterization, and proteomic analysis, will elucidate how similar functional materials differentiate themselves either through chemical or structural modifications to fulfill specific photonic purposes.

4. Experimental Section

Spectral Reflectance Measurements and Physiology Studies: Spectrometers (Ocean Optics, FL, USA; USB2000, sensitive in the UV and visible wavebands; QE65000, sensitive in UV, visible and IR wavebands) were used to quantify optical properties of fin spots (containing leucophores). Measurements shown in Figure 2 were taken using a 1 mm fiber optic cable linked to a stereo microscope (Zeiss; incident light angle ca. 10 degrees). The angular measurements shown in Figure 2B were obtained using a clear custom-made goniometer. This allowed movement of the fin spot sample in three dimensions. The actual measuring direction is vertical, given by position of the microscope. Measurements shown in Figure 1B,ii were taken using a reflectance probe (QR200-7-UV-VIS, Ocean Optics; i.e., normal incidence measurement; no microscope to avoid absorbance in UV and IR) and a broadband light source (HPX-2000, Ocean Optics; spectral output: 185–2000 nm) to measure an area of 1–2 mm^2. All measurements were normalized to a white Lambertian reflectance standard (WS-1, Ocean Optics, >98% reflective from 250–1500 nm). Reflectance measurements are given in percent reflectance relative to this white standard (see e.g.,[32,37–39]). Simulation results (discussed below) suggest that leucophore-containing fin spots reflect light similar to a Lambertian surface. Relative reflectance measurements, measured at specified angles, were used as representative measurements. Physiological activation of leucophores of the fin spot was tested. Small pieces of skin (approximately 10 mm^2) were pinned onto Sylgard in 35 mm Petri dishes containing cooled artificial seawater (ASW, in mM: NaCl 470, KCl 10, $CaCl_2$ 10, $MgCl_2$ 60, Hepes 10, pH 7.8). Pharmacological solutions, freshly made up in ASW, were applied directly to the skin by pipette after the ASW had been removed. Acetylcholine (Ach; 1×10^{-4} M), L-glutamate (L-glu; 1×10^{-3} M), serotonin (5-HT; 1×10^{-4} M), potassium chloride (KCl; 3×10^{-3} M) and noradrenaline (Nor; 1×10^{-3} M) were applied separately to skin (all chemicals were purchased from Sigma, USA). Reflectance spectra were taken at 0 min, 3 min, 5 min and 10 min after drug administration (Figure S1, Supporting Information).

Morphology Studies: Fin spots were fixed in a modified Karnovsky's fixative,[40] post-fixed in 1% osmium tetroxide, and embedded in epoxy. For light microscopy, sections (1 µm thickness) were cut, stained as outlined in Results, and viewed on a Zeiss Axioskop. For SEM, fixed and dehydrated tissue pieces were dried using hexamethyldisilazane (HMDS; Sigma), mounted on aluminum stubs, sputter-coated lightly with platinum, and examined using a Zeiss Supra 40VP SEM. For 3D analysis, fin dermis was dissected, and 1 cm^2 pieces were fixed as above. The aldehyde-fixed samples were post-fixed using OTO (osmium–thiocarbazide–osmium) regime,[41,42] en bloc stained with heavy metals (uranyl acetate, Walton's lead aspartate), and embedded in Epon-Araldite.[43] Trimmed blocks were sent to Mr. Joel Mancuso (Gatan Inc., Pleasanton, CA) for processing and image acquisition using their 3View serial block-face scanning electron microscopy system, which involved serially sectioning (50 nm) an epoxy embedded fin spot and, using high resolution SEM, collecting images of the block face after each section was removed.

The resulting 1500 images (2048 × 2048, 16-bit, with isotropic image resolution of 50 nanometers per pixel) contained a 3D field of leucophores and iridophores. The principal interest was to investigate the distribution of leucosomes within a single leucophore. From this data set, we selected a 3D region (1024 × 1024 × 750, 8-bit), which completely encompassed one leucophore that, by observation, contained almost exclusively spherical leucosomes. Although the outer cell membranes could not be definitely resolved, the cell's 3D boundary was distinguishable by abrupt changes in tissue characteristics (areas of spheres versus platelets). Regions exclusive of the cell of interest were erased manually. The targeted leucophore contained ≈12 000 leucosomes (Figure 3C) that were uniformly distributed within its volume of approximately 11 000 μm^3 (Figure S2, Supporting Information). The leucosome size distribution was obtained using a custom-made algorithm, in which each voxel brighter than an interactively set threshold was evaluated in terms of being central to a leucosome. Axial rays from each voxel extended outward in numerous directions and terminated when they encountered an edge (an adaptive function of the initial candidate voxel's intensity). Only voxels located at spheroid centers generated oppositely directed rays of approximately similar length for every direction. Thus, an x,y,z voxel coordinate and a radius (taken as the average length of the six rays on the cardinal axes) was generated for each leucosome meeting the designated constraints. This computation located most of the leucosomes in the cell (Figure 3C).

Holographic Microscopy: Fin spot samples were prepared by dissociating the fin skin of *S. officinalis* using collagenase (Sigma-6; 6 mg/mL of buffered sea water, shaken overnight at 4–6 °C). Individual fin spots containing leucophores were harvested and washed in buffered sea water, and placed on microscope slides where individual cells could be identified. The holographic characterization setup is based on an inverted microscope (Nikon Ti) equipped with an oil immersion objective (Nikon 100× 1.3 NA Plan Fluor). A fiber coupled 635 nm diode laser (Thorlabs) was collimated, passed through a linear polarizer and directed onto the samples so that the optical axes of the collimator and microscope objective were aligned. The out-of-focus holograms resulting from the interference of directly propagating light with light scattered by individual leucosomes were collected with the 100× objective, cascaded with a 1.5× magnification tube lens, and imaged with a 13 µm × 13 µm pixel CCD camera (Princeton Instrument ProEM512). Multiple image frames of freely diffusing leucosomes were recorded, and each frame

was normalized to the average of all images acquired at that same position to minimize the effects of intensity variations due to laser speckle patterns and other artifacts. The resulting normalized holograms were fit to Lorenz-Mie theory using software developed by the Grier lab.[22–24,26] The free fitting parameters were the particle's 3D position, radius, refractive index, and a constant alpha value that accounts for laser illumination intensity variations at different particle positions. Prior to leucosome measurements, the holographic technique and setup were validated by verifying the particle size and refractive index of NIST traceable polystyrene microspheres (NT15N/10550, Bangs Laboratories, Inc.).

Simulations: As discussed in the morphological results of the fin spot, measured reflectance is the contribution of both iridophores and leucophores. To date, the morphological characteristics of iridophores in the fin spot system remain unquantified. In the numerical simulations, the scattering properties of a single leucosome were first calculated, and Monte Carlo simulations for the multiple scattering from a collection of leucosomes were used to obtain the diffuse reflectance spectrum. This simulated spectrum was compared with fin spot measurements; the difference was inferred to be the contribution of iridophore plates to the reflectance spectrum.

The individual leucosomes shown in Figure 3 are highly spherical and were modeled as solid spheres. The electromagnetic scattering of such a leucosome can be solved efficiently by Lorenz-Mie theory.[44] The resulting polarized scattering properties are represented by the Mueller matrix,[44] which contains all the optical information that can be obtained from a particle or particles undergoing elastic scattering. To account for the size variations of leuosomes within a realistic system, the Mueller matrix was averaged according to the measured size distribution obtained from the Gatan 3 View electron microscopy data (Figure 3D). The average refractive index value measured by the holographic microscopy was used to model the particle index ($n_p = 1.51$) while the interstitial medium was assumed to be close to water ($n_m = 1.33$).

The spatial structure of a leucophore can influence whether the scattering between leucosomes is coherent or incoherent and thus will require distinct methods to simulate them. For coherent scattering, such as in systems with short-range order,[12,28,29] it can act in such a way to preserve the phase relations between scatter events; for incoherent scattering, where the scatterer positions are random, the phase relations become irrelevant and the scatterers act independently.[7] We analyzed the measured leucosome coordinates using a 2D discrete Fourier transformation (DFT),[29] and found that there are no prominent peaks in the spatial power spectrum other than at the origin point with zero spatial frequency (Figure S6, Supporting Information). Leucosomes are distributed uniformly along all three cardinal axes (Figure S2, Supporting Information). From this analysis, we inferred that there is no apparent periodic structure for leucosome positions and that a leucophore can be treated as a random system. A Monte Carlo method, which is designed for such a random system with incoherent multiple scattering, was used to simulate the diffuse reflectance.

The overall geometry of the system was approximated by a finite thickness, infinitely wide slab. This approximation was based on the setup of the reflectance measurement, where the spectral reflectance was measured on a large skin area around 1×1 mm^2. Comparatively, the system thickness (L) of an entire fin spot, made up of many reflective cells, can be as thin as 100 μm. In the simulations, a beam of directional light is incident on this system with several incident angles commensurate with the measurements in Figure 2.

Leucophore reflectance depends on both the average number density of its constituent leucosomes (n_d) and the system thickness (L). These two quantities work together as a product, $n_d L$, to influence the system reflectance. For the Monte Carlo method, the incident light was treated as a sequence of photon packets. The propagation distances of a photon packet were sampled for each scattering process using the Bouguer-Lambert-Beer law, and the scattering directions were sampled using the phase functions calculated from Lorenz-Mie theory[45] Various variance reduction methods were used to increase the accuracy. The statistical summation of the photon trajectories was used to estimate the polarized diffuse reflectance for the bulk system.

Protein Analysis: Dissected fin spots were disrupted in extraction buffer (Tris-HCl, pH 8, 100 mM NaCl, 1 mM benzamidine, 0.5 mM PMSF, 0.1% Triton X-100) using a Dounce homogenizer. The extract was then centrifuged at 10 000 rpm for 5 min where the white leucophore material was pelleted. Leucophore pellets were washed three times with extraction buffer before being resuspended in extraction buffer for future analysis. Resuspended leucophore cell pellets were solubilized by boiling in SDS-PAGE sample buffer followed by electrophoretic resolution with SDS-PAGE using Tricine running buffers.[46] Protein bands of interest were excised from Coomassie-stained gels, digested with trypsin, and sequenced by MS/MS fragmentation on an AB Sciex 4800 MALDI-TOF/TOF instrument as described previously.[47] Briefly, peptide digestions were diluted 1:1 in freshly prepared matrix solution (5 mg/mL α-Cyano-4-hydroxycinnamic acid in 60% acetonitrile/0.1% formic acid/5 mM ammonium monobasic phosphate) and spotted onto the target plate. Spectra were collected in reflector positive ion mode using the AB Sciex 4000 Explorer acquisition software ver 3.5.1. Alternatively, proteins resolved by Tricine SDS-PAGE were blotted onto nitrocellulose membranes for Western blot analysis. Blotted membranes were probed with a rabbit polyclonal antibody directed against reflectins from the Hawaiian bobtail squid (*Euprymna scolopes*)[34] followed by probing with a biotinylated goat anti-rabbit secondary antibody and an alkaline phosphatase-conjugated streptavidin for colorimetric detection. To obtain highly-enriched but rarified leucophore samples, fin spots were dissociated in collagenase (type VI, Sigma). Isolated cells were placed on PET membrane slides (Zeiss), catapulted into the caps of centrifuge tubes using a laser capture micro-dissection system (Zeiss-PALM; 40× objective), and frozen in liquid nitrogen. Cells were then boiled directly in SDS-PAGE sample buffer, without prior centrifugation, and subjected to Western blot analysis. Protein analysis of soluble and insoluble fin spot extracts was carried out using a Bradford protein assay (Bio-Rad, Hercules, CA), per manufacturer's instructions, where the insoluble extract was first solubilized in 1 N NaOH at room temperature before analysis.

Leucophore peptides were compared to known sequences using blastp at the National Center for Biotechnology Information (http://blast.ncbi.nlm.nih.gov/). Since many of the peptides matched to multiple *S. officinalis* reflectins, all *S. officinalis* reflectin sequences available in GenBank were aligned using Clustal Omega (1.1.0). Leucophore peptides that matched were mapped onto the sequence (Figure S4, Supporting Information).

Supporting Information

Supporting Information is available from the Wiley Online Library or from the author.

Acknowledgements

The authors are grateful for primary funding from the Air Force Office of Scientific Research (AFOSR grant FA9550-09-0346) and the Office of Naval Research (ONR BRC grant N00014-10-1-0989 to RTH and ONR MURI grant N00014-09-1-1054 to GK). Additional funding was provided to MBL authors by the Defense Advanced Research Project Agency (DARPA DSO grant W911NF-10-1-0113), and Army Research Laboratory (ARL grant W911NF-09-2-0043), and to GK by National Science Foundation (OCE-1130906). The authors thank Elizabeth Kripke for the 3D rendering of the leucophore in Figure 3C, Dr. John B. Messenger for initial physiology experiments, and Mr. Joel Mancuso at Gatan, Inc. for generating the serial block-face scanning electron microscopy images. They also thank Dr. Jason Heikenfeld (Univ. of Cincinnati) for helpful discussions, Dr. Margaret McFall-Ngai (Univ. of Wisconsin-Madison)

for the anti-reflectin antibody, and Professor Kenneth Greis (Univ. of Cincinnati) for mass spectrometry analyses.

Received: December 14, 2012
Revised: February 5, 2013
Published online: April 2, 2013

[1] G. Wyszecki, W. S. Stiles, *Color Science: Concepts and methods, quantitative data and formulae*. 2nd ed. John Wiley & Sons, Inc., New York **1982.**
[2] H. B. Cott, *Adaptive Coloration in Animals*, Methuen & Co., Ltd., London **1940**.
[3] R. T. Peterson, V. M. Peterson, *A Field Guide to the Birds of Eastern and Central North America*. 5th ed, Houghton Mifflin Company, Boston **2002**.
[4] P. Vukusic, B. Hallam, J. Noyes, *Science,* **2007**, *315*, 348.
[5] D. G. Stavenga, S. Stowe, K. Siebke, J. Zeil, K. Arikawa, *Proc. R. Soc. B* **2004**, *271*, 1577.
[6] S. Yoshioka, S. Kinoshita, *Proc. R. Soc. B* **2006**, *273*, 129.
[7] S. M. Luke, B. T. Hallam, P. Vukusic, *Appl. Opt.* **2010**, *49*, 4246.
[8] R. T. Hanlon, J. B. Messenger, *Philos. Trans. R. Soc. B.* **1988**, *320*, 437.
[9] J. Allen, L. M. Mäthger, A. Barbosa, R. T. Hanlon, *J. Comp. Physiol. A* **2009**, *195*, 547.
[10] D. Froesch, J. B. Messenger, *J. Zool. London* **1978**, *186*, 163.
[11] A. R. Parker, V. L. Welch, D. Driver, N. Martini, *Nature* **2003**, *426*, 786.
[12] B. Q. Dong, X. H. Liu, T. R. Zhan, L. P. Jiang, H. W. Yin, F. Liu, J. Zi, *Opt. Express* **2010**, *18*, 14430.
[13] G. H. Gelinck, H. E. A. Huitema, M. van Mil, E. van Veenendaal, P. J. G. van Lieshout, F. Touwslager, S. F. Patry, S. Sohn, T. Whitesides, M. D. McCreary, *J. Soc. Inf. Display* **2006**, *14*, 113.
[14] D. H. Kim, N. S. Lu, R. Ma, Y. S. Kim, R. H. Kim, S. D. Wang, J. Wu, S. M. Won, H. Tao, A. Islam, K. J. Yu, T. Kim, R. Chowdhury, M. Ying, L. Xu, M. Li, H.-J. Chung, H. Keum, M. McCormick, P. Liu, Y.-W. Zhang, F. G. Omenetto, Y. Huang, T. Coleman, J. A. Rogers, *Science* **2011**, *333*, 838.
[15] S. A. Morin, R. F. Shepherd, S. W. Kwok, A. A. Stokes, A. Nemiroski, G. M. Whitesides, *Science* **2012**, *337*, 828.
[16] E. Kreit, L. M. Mäthger, R. T. Hanlon, P. B. Dennis, R. R. Naik, E. Forsythe, J. Heikenfeld, *J. R. Soc. Interface* **2012**, doi: 10.1098/rsif.2012.0601.
[17] M. Hagedon, S. M. Yang, A. Russell, J. Heikenfeld, *Nature Commun.* **2012**, DOI:10.1038/ncomms2175.
[18] R. Fujii, H. Kasukawa, K. Miyaji, *Zool. Sci.* **1989**, *6*, 477.
[19] K. M. Cooper, R. T. Hanlon, B. U. Budelmann, *Cell Tissue Res.* **1990**, *259*, 15.
[20] J. B. Messenger, *Biol. Rev.* **2001**, *76*, 473.
[21] C. P. Song, P. Wang, H. A. Makse, *Nature* **2008**, *453*, 629.
[22] S. H. Lee, Y. Roichman, G. R. Yi, S. H. Kim, S. M. Yang, A. van Blaaderen, P. van Oostrum, D. G. Grier, *Opt. Express* **2007**, *15*, 18275.
[23] F. C. Cheong, K. Xiao, D. J. Pine, D. G. Grier, *Soft Matter* **2011**, 7, 6816.
[24] F. C. Cheong, K. Xiao, D. G. Grier, *J. Dairy Sci.* **2009**, *92*, 95.
[25] T. M. Jordan, J. C. Partridge, N. W. Roberts, *Nat. Photonics* **2012**, *6*, 759.
[26] J. C. Crocker, D. G. Grier, *J. Colloid Interface Sci.* **1996**, *179*, 298.
[27] S. S. Spicer, D. B. Meyer, *Am. J. Clin. Pathol.* **1960**, *33*, 453.
[28] H. Noh, S. F. Liew, V. Saranathan, S. G. J. Mochrie, R. O. Prum, E. R. Dufresne, H. Cao, *Adv. Mater.* **2010**, *22*, 2871.
[29] R. O. Prum, R. H. Torres, S. Williamson, J. Dyck, *Nature* **1998**, *396*, 28.
[30] J. Zi, X. Yu, Y. Li, X. Hu, C. Xu, X. Wang, X. Liu, R. Fu, *Proc. Natl. Acad. Sci. USA* **2003**, *100*, 12576.
[31] N. G. Jerlov, *Marine Optics*, Elsevier, Amsterdam **1976**
[32] L. M. Mäthger, E. J. Denton, N. J. Marshall, R. T. Hanlon, *J. R. Soc. Interface* **2009**, *6*, S149.
[33] A. L. Holt, A. Sweeney, S. Johnsen, D. E. Morse, *J. R. Soc. Interface* **2011**, *8*, 1386.
[34] W. J. Crookes, L. Ding, Q. L. Huang, J. R. Kimbell, J. Horwitz, M. J. McFall-Ngai, *Science* **2004**, *303*, 235.
[35] R. M. Kramer, W. J. Crookes-Goodson, R. R. Naik, *Nat. Mater.* **2007**, *6*, 533.
[36] F. G. Omenetto, D. L. Kaplan, *Science* **2010**, *329*, 528.
[37] A. Springsteen, *Anal. Chim. Acta* **1999**, *380*, 379.
[38] M. D. Shawkey, A. M. Estes, L. M. Siefferman, G. E. Hill, *Proc. R. Soc. London B* **2003**, *270*, 1455.
[39] G. Zonios, A. Dimou, *Opt. Express* **2008**, *16*, 8263.
[40] A. M. Kuzirian, E. Meyhöfer, L. Hill, J. T. Neary, D. L. Alkon, *J. Neurocyol.* **1986**, *15*, 629.
[41] A. M. Seligman, H. L. Wasserkrug, J. S. Hanker, *J. Cell Biol.* **1966**, *30*, 424.
[42] R. O. Kelley, R. A. Dekker, J. G. Bluemink, *J. Ultrastruct. Res.* **1973**, *45*, 245.
[43] C. W. Geiselman, C. N. Burke, *J. Ultrastruct. Res.* **1973**, *43*, 220.
[44] C. F. Bohren, D. R. Huffman, *Absorption and Scattering of Light by Small Particles*, Wiley-VCH Verlag GmbH, Weinheim, Germany **2007**.
[45] P.-W. Zhai, G. W. Kattawar, P. Yang, *Appl. Opt.* **2008**, *47*, 1037.
[46] H. Schägger, G. von Jagow, *Anal. Biochem.* **1987**, *166*, 368.
[47] T. Eismann, N. Huber, T. Shin, S. Kuboki, E. Galloway, M. Wyder, M. J. Edwards, K. D. Greis, H. G. Shertzer, A. B. Fisher, A. B. Lentsch, *Am. J. Physiol. Gastrointest. Liver Physiol.* **2008**, *296*, G266.
[48] R. T. Hanlon, J. B. Messenger, *Cephalopod Behaviour*, Cambridge University Press, Cambridge **1996**.
[49] L. M. Mäthger, R. T. Hanlon, *Biol. Lett.* **2006**, *2*, 494.
[50] L. M. Mäthger, R. T. Hanlon, *Cell Tissue Res.* **2007**, *329*, 179.